Research Article

Zhao Lingling* and Jon Knepper

Analysis of the Imaging Characteristics of the KB and KBA X-ray Microscopes at Non-coaxial Grazing Incidence

https://doi.org/10.1515/phys-2018-0094
Received Aug 23, 2018; accepted Sep 19, 2018

Abstract: In the last 20 years, requirements for x-ray lithography, space technology and ICF process diagnosis, the x-ray imaging technology has been developed. However, x-ray imaging turns out to be more difficult due to intense absorption of x-rays, and the refractive index of x band is slightly less than 1. Normal imaging method may not be suitable for x-ray band. At present, grazing reflective imaging and coded aperture imaging are commonly used for this band. This paper presents a detailed analysis of the imaging characteristics of single-mirror and double-mirror. Then the focal distance, field obliquity and aperture position of the mirrors of the KBA microscopes at grazing incidence are studied. The results show that the structure arrangement of the KBA microscope is rather reasonable, and can be considered as theoretical evidence in the design and manufacture of KBA microscopes.

Keywords: x-ray imaging, KBA microscope, grazing incidence, anastigmatic system

PACS: 81.15.Cd, 42.82.Cr

1 Introduction

Since the refractive index of a medium to x-ray is less than 1 and the intense medium absorption, the x-ray imaging becomes difficult. Normal imaging methods are not suitable for the x-ray band. Mostly used technologies use the grazing incidence imaging and the coded aperture imaging [1–4] methods. In 1922, Compton discovered total external reflection phenomenon of x-rays when reflected from a polished surface at gazing incidence [5], which laid the basis for x-ray grazing imaging.

In 1948, Kirkpatrick and Baez proposed a method eliminating astigmatism involving a single concave mirror at grazing incidence [6]. In this method, two spherical or cylindrical mirrors are placed orthogonally, which is also known as the KB microscope. Although astigmatism is eliminated, severe field obliquity and geometric aberrations are introduced and spherical aberration is left uncorrected. With smaller grazing angle, the situation becomes more complicated. Therefore, the KB microscopes failed to draw much attention of scholars for a time.

Since 1990s, the requirements of x-ray photo lithography, space technology, high energy physics and ICF process diagnosis are on the increase, resulting in rapid development of x-ray imaging [7–13]. KB microscopes caught the attention of researchers again.

In 1997, R. Saunenf el al.in France developed a KBA x-ray microscope. The difference between the KBA and KB microscope is the employs a single-mirror while the KBA microscope uses a double-mirror system. The KBA microscope converges the beams on the same plane with two spherical mirrors arranged in “parallel” rows at a certain angle, which reduces the tilt of the image plane. Thus, the imaging quality of the off-axis points is proved, enlarging the range of the field.

This paper analyzes the imaging characteristics of single-mirror and double-mirror microscopes at grazing incidence. Then the focal distance, field obliquity and aperture potion of the mirrors of KBA microscopes at grazing incidence are studied. The results show that the structure and arrangement of KBA microscope is rather reasonable and can be considered as the theoretical evidence in the design and manufacture of KBA microscopes.

***Corresponding Author: Zhao Lingling:** School of Information and Electrical Engineering Ludong University, Yantai, Shandong 264025, China; Email: Zll765200@163.com
Jon Knepper: Institute of Engineering, Rensselaer Polytechnic Institute, Troy, New York, 12180, United States of America

2 The characteristics of the KB and KBA microscopes

2.1 Imaging characteristics of single-mirror

2.1.1 Spherical aberration

The KB microscope can be regarded as a simple single mirror system. The meridian and sagittal plane are composed of single concave spherical (or cylindrical) mirrors, respectively. The following discusses the method of reducing the spherical aberrations. For small enough aperture u and grazing angle θ, the longitudinal aberration Δ is (shown as figure 1) [5, 6].

$$\Delta = \Delta(u', l', r, \theta) \approx -\frac{3u'l'^2(r\theta - l')}{r^2\theta^3}$$
$$\Rightarrow \Delta = 3/4u'(M-1)(M+1)l'/\theta$$

Where, l, l' are the object distance OP and image distance PO', respectively. θ is the grazing angle. M is the magnifying power. u' is the aperture angle. R is the curvature radius.

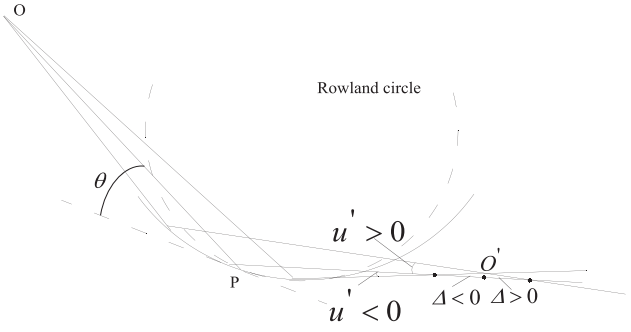

Figure 1: spherical aberration of a single concave mirror

Then the optimal resolution ϕ_{opt} can be defined as:

$$\phi_{opt} = 3^{5/6}\left(\frac{\kappa}{32}\frac{l}{\theta}\lambda^2\right)^{1/3}$$

Where, λ is the operation wavelength; l is the distance from the target to the first mirror, namely the working distance (Wd). Considering proper manufacturing and installation error, the value of κ can be reasonably determined as 5/2. As the quality of off-axis imaging always decreases with enlarging the field of view, the optimal resolution is only suitable for the points on axis. However, it indeed gives the optimal imaging quality formula for the single-mirror KB system, supposing the off-axis aberration is small. The resolution defined by this formula takes into account the joint effect of the diffraction and geometric dispersion. Therefore, the optimal resolution ϕ_{opt} reflects the following relationship:

$$\phi_{opt} \propto \left(l\lambda^2/\theta\right)^{1/3}$$

Namely, ϕ_{opt} is proportional to $\left(l\lambda^2/\theta\right)^{1/3}$. The single-mirror can be refined by increasing Wd and the grazing angle. The value of l is defined by this rule: the device should be free of the damage of the laser beams reaching the target sphere and the unvaporized fragments; θ is decided by the maximum grazing angle reflecting the x rays.

Because the maximum grazing angle $\theta_{\max}$ is proportional to λ, and the angle could be at least three times larger or more larger for multilayer film surfaces, this formula is still suitable. Therefore, ϕ_{opt} is proportional to $l^{1/3}\lambda^{1/3}$.

As it can be seen, the smaller the working distance is, the higher the energy of x rays will have, resulting in better imaging quality.

Although the above formula only describes the imaging situation of the single-mirror KB microscope, it can serve as a reference for the design of double-mirror systems.

2.1.2 Field obliquity

This section analyzes the imaging on the meridian plane of the single-mirror, as shown as figure 2. AB is a line on the meridian plane. O is the apex of the mirror. θ_A and θ_B are the grazing angle of beams AO and BO respectively. The included angle $\angle AOB$ is denoted as $\Delta\theta$. A' and B' are the real image positions of A and B, respectively. P' is the image plane. Here, we regarded B'', the projection of point B' on plane P', as the image point of point B (In fact, B'' is a dispersion spot).

$AO = l_A$, $BO = l_B$, $OA' = l'_A$, $OB' = l'_B$. The meridian focal distance of the single-mirror at grazing incidence can be obtained by Young's formula, imaging from the narrow beam adjacent to the primary ray on the meridian plane. Young's formula within the meridian plane is:

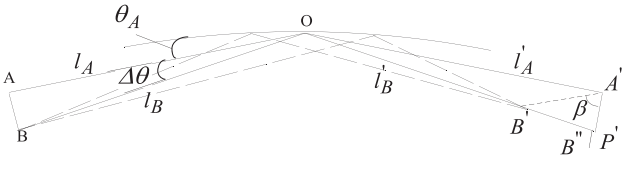

Figure 2: Image of single-mirror

$$\frac{n'\cos^2\theta'_p}{l'} - \frac{n\cos^2\theta_p}{l} = \frac{n'\cos\theta'_p - n\cos\theta_p}{r} \tag{1}$$

Where, l and l' are the object distance and image distance of the meridian ray, respectively. θ_p, θ'_p are the incidence angle and refraction angle of the primary ray, respectively. n and n' are the refractive indexes of the incidence and exit medium, respectively and r is the radius of curvature. When the target approaches to infinity, $l \to \infty$. Assuming the incidence angle is θ, $\theta = 90^\circ - \theta_p$, $\theta'_p = \theta_p$ and $n' = -n = -1$. The following equation can be obtained from formula (1):

$$l' = \frac{r\sin\theta}{2} \tag{2}$$

$$f'_t = l' = \frac{r\sin\theta}{2} \approx \frac{r\theta}{2} \tag{3}$$

$$\varphi = \frac{1}{f'_t} = \frac{2}{r\sin\theta} \tag{4}$$

As it can be seen, the meridian focal distance of the single-mirror at grazing incidence is a function of the incidence angle θ. According to the Gauss formula:

$$\frac{1}{l'} - \frac{1}{l} = \frac{1}{f'_t} \qquad \text{it yields} \qquad l' = \frac{l \times f'_t}{l + f'_t}$$

For point A and point B, the following equations are obtained.

$$l'_A = \frac{l_A \times f'_A}{l_A + f'_A}, \quad l'_B = \frac{l_B \times f'_B}{l_B + f'_B} \tag{5}$$

f'_A, f'_B are the meridian focal distances of the incidence angles θ_A, θ_B, respectively. For the case when $\Delta\theta$ is very small, $l_A \sim l_B$. In order to avoid severe plane obliquity, it is necessary to make $l'_A \approx l'_B$. As it can be seen from formula (5), $f'_A \approx f'_B$ is necessary as well. As it can be known from formula (3)(r is large), the meridian focal distance is a function of the incidence angle θ for the single -mirror. As the meridian focal distance varies strongly with the variation of θ, the condition $f'_A \approx f'_B$ is not satisfied, resulting in serious image plane obliquity for the single-mirror.

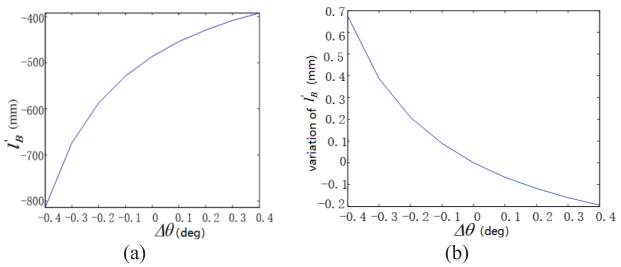

Figure 3: Image distance and altering of single-mirror

An example of the imaging of a single-mirror is provided. Assuming there are two points A and B in the object space; $A'$and B' are the respective image points; the grazing angle of point A is 1.6^0.

If the working distance of point A and B are both -220 mm, when $\Delta\theta$ varies in the range of $-0.4^\circ \sim +0.4^\circ$, as it can be known from formula (5), $l'_A = -481.8141$ mm and l'_B varies in the range of $-798.497 \sim -389.205$ mm(see figure 3(a)). As l'_B varies more slightly in the case of $\Delta\theta > 0$ compared to $\Delta\theta < 0$, the field obliquity will be less (see figure 3(b)).

2.2 Imaging characteristics of double-mirror

2.2.1 Field obliquity

The KBA microscopes mainly converge light beams onto the meridian plane of the double-mirror. The focal distance of the meridian plane is derived below.

The double-mirror is composed of two single-mirrors, shown as figure 4. Q_1 and Q_2 are the apexes of mirrors M_1 and M_2, respectively. A' and B' are the image points of A and B, respectively. Because the radii of the mirrors are large, we could regard the mirrors as plane mirrors in the analysis of focal distance. Then it yields $\theta'_A = \eta - \theta_A$. As before, to avoid serious image plane obliquity, it is required that the focal distance to stay constant.

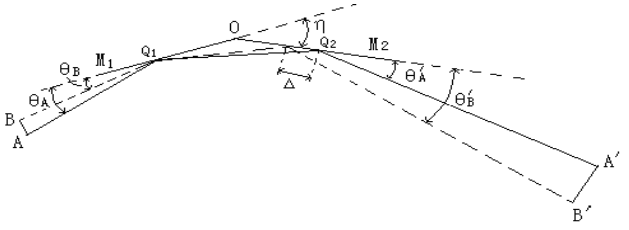

Figure 4: Image of double-mirror

For the double-mirror with included angle η, we can derive the focal distance at grazing angle θ. The focal distance of the double-mirror can be obtained by

$$\varphi = \varphi_1 + \varphi_2 - d\varphi_1\varphi_2 \tag{6}$$

When $r_1 = r_2 = r$,

$$\varphi_1 = \frac{2}{r\sin\theta}, \qquad \varphi_2 = \frac{2}{r\sin(\eta - \theta)}$$

d is the center-to-center spacing of the two mirrors. η is the included angle of the two mirrors.

$$\varphi = \frac{2}{r\sin\theta} + \frac{2}{r\sin(\eta - \theta)} - \frac{4d}{r^2\sin\theta\sin(\eta - \theta)} \tag{7}$$

When θ, $(\eta - \theta)$ is a very small, $\sin\theta = \theta$, $\sin(\eta - \theta) = \eta - \theta$. The above formula becomes

$$\varphi = \frac{2}{r\theta} + \frac{2}{r(\eta - \theta)} - \frac{4d}{r^2\theta(\eta - \theta)} = \frac{2r\eta - 4d}{r^2\theta(\eta - \theta)} \tag{8}$$
$$f' = \frac{1}{\varphi} = \frac{r^2\theta(\eta - \theta)}{2r\eta - 4d}$$

As it can be seen from the above formula, for given η, the focal distance f' is a function of the incidence angle θ. Differentiating both sides of the above formula, it yields

$$df' = \frac{r^2(\eta - 2\theta)}{2r\eta - 4d} \cdot d\theta \tag{9}$$

When $\theta = \frac{\eta}{2}$, the first-order derivative of f' is 0 and f' obtains the extreme value. $\theta = \frac{\eta}{2}$ is a stationary point, within the neighbourhood of which, f' hardly varies with θ, namely $\frac{df'}{d\theta} = 0$. This indicates, the image plane will not slant in the neighbourhood of point $\theta = \frac{\eta}{2}$. At this time, the focal distance of the double-mirror is

$$f' = \frac{r\eta}{8(1 - \frac{2d}{r\eta})} \tag{10}$$

When $d << r\eta$,

$$f' \approx \frac{r\eta}{8} \tag{11}$$

In reverse, when the incidence angles on the pseudo-axis are known, the included angles of the double-mirror can be calculated. Namely, $\eta = 2\theta$. In this way, the image planes of the points on the axis will not slant. But for the points off axis, the incidence angle θ has been changed while η remains unchanged, so $\eta \neq 2\theta$, $\frac{df'}{d\theta} \neq 0$. Thus, the focal distance varies with θ, resulting in image plane obliquity.

Next, Matlab was adopted to simulate the effects of incidence angle θ and included angle ηon the focal distance of the double-mirror. The focal distance can be calculated according to formula (9). The radius r is 29000 mm in this case. For double-mirrors with different included angles (η), we plot the curves of the focal distance with respect to the incidence angle θ, shown as figure 5(a), (b) and (c).

Figure 5(a), (b) and (c) show the curves of the focal distance f varying with the incidence angle θ when the included angles of the double mirror η are 3°, 3.2° and 3.4°, respectively. Figure (d) shows the curve of the focal distance of one mirror composed of the double-mirror varying with θ. As it can be seen from figure (a), (b) and (c), when the included angle of the double-mirror changes, the focal distance of the double-mirror will change. For different η, the extreme value is when $\theta = \frac{\eta}{2}$. Moreover, compared to the focal distance of the single-mirror (figure 4(d)), the focal distance of the double-mirror varies in a smaller range with θ. As it can be known from formula (5), the reduction of f'_A, f'_B reflects image obliquity will decrease by using the double-mirror structure. According to the imaging characteristics of the single-mirror, the imaging quality will be better with bigger incidence angle. And for the double-mirror system, the difference of the incidence angles on the two mirrors should be possibly smaller, namely approaching to $\frac{\eta}{2}$.

2.2.2 Determination of the position of the aperture

The use of aperture can decrease the aberration of the off-axis beams and improve the spatial resolution. For the limitation of space, the aperture of the KBA microscope can only be placed on the mirrors. For the double-mirror system, the aperture can be placed either at the first mirror or the second mirror.

To disclose the effect of the aperture on imaging quality, a double-mirror system (Figure 5) was constructed with the following parameters: object distance = −220 mm, image distance = 1, 856 mm, solid angle 4×10^{-6} sr; centre-to-centre distance of the two mirrors = 27 mm, and incidence angle of each mirror = 1.6°.

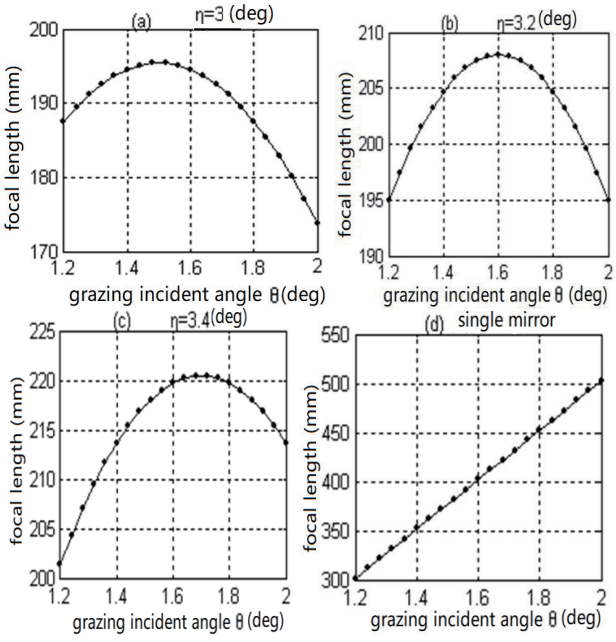

Figure 5: Curve of focal distance with respect to incidence angle

Taken the first mirror for an example, the relationship between the aperture angle and the solid angle is

$$u = \sqrt{\frac{\omega_a}{\pi}} = \sqrt{\frac{4 \times 10^{-6}}{3.1416}} = 1.128 \times 10^{-3}$$

The approximate size of the mirror can be calculated on this basis (see figure 6).

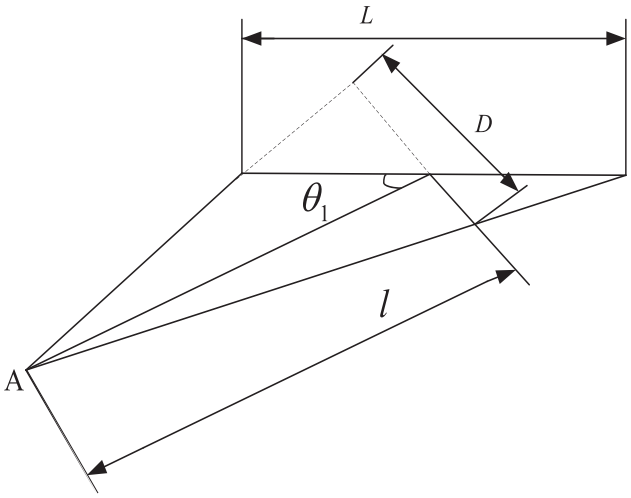

Figure 6: Relationship between the aperture and the size of the mirror

$$L = \frac{D}{\sin\theta_1} = \frac{2lu}{\sin\theta_1} = \frac{2\times(-220)\times\left(-1.128\times10^{-3}\right)}{\sin(1.6^\circ)} \approx 18\ \text{mm}$$

This is just the aprproximate size of the points on the axis. The practical calculation is more complicated. Therefore, considering the points off the pseudo-axis, the size of the first mirror is bigger than the calcualted result.

By calculation, when the aperture is at the first mirror, the length of the first mirror is 26.408 mm and the second is 41.060 mm. And when the aperture is at the second mirror, the length of the first mirror is 39.482 mm and the second is 27.066 mm. Therefore, the structure is more compact by placing the aperture on the second mirror compared to placing it on the first. One of the mirrors of the double-mirror system is relatively longer, so as not to lose the light beams in the whole field view, which is called as the field mirror and the other is the aperture mirror.

As it can be seen from figure 7, when the aperture is placed at the first mirror and the second respectively, the difference of blur is very small if the field view is positive otherwise the former has much bigger blur than the later.

Figure 8 shows the field angles when placing the aperture at the first mirror and the second mirror. As it can be seen, the field angles present no big differences for both mirrors in the whole field. But when the aperture is placed at the first mirror, the field angles for both mirrors present greater variation compared to placing it at the second mirror.

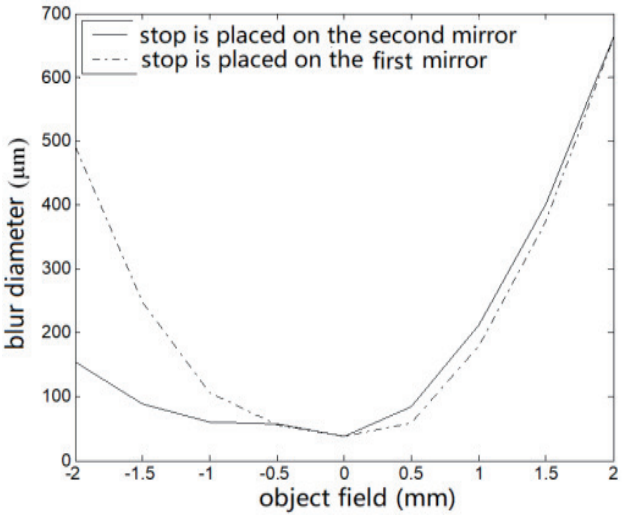

Figure 7: Blur of aperture located on either mirror

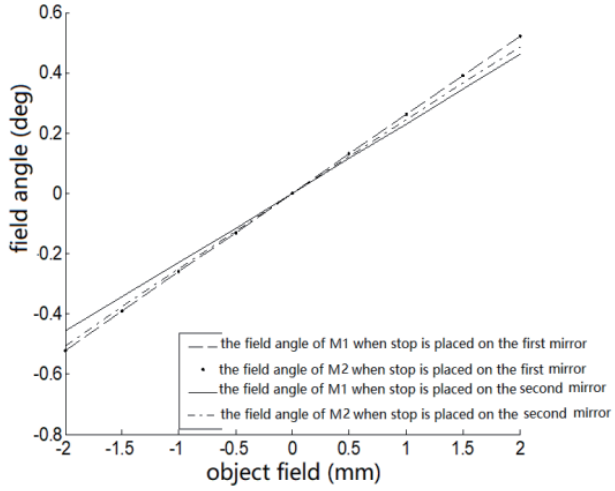

Figure 8: Field angle of aperture located on either mirror

As it can be known from the above analysis, placing the aperture at the second mirror is a better solution compared to placing it on the second one. Therefore, the apertures of the meridian plane and the sagittal plane are separately placed in this system. Namely, the aperture of the meridian plane is placed at the second mirror and the aperture of the sagittal plane is placed at the forth mirror.

3 Conclusion

This paper compares the imaging characteristics of the single-mirror and double-mirror system at grazing incidence. Then the focal distance and filed obliquity of the KBA microscopes at grazing incidence are studied. The structure of the KBA microscopes are analyzed and proved

to be reasonable. The results show when the incidence angle is half of the included angle of the double-mirror, the filed obliquity of the double-mirror is the least, and it is optimal to place the aperture at the second mirror rather than the first mirror from the perspective of imaging quality.

References

[1] Chkhalo N. I., Gaikovich P. K., Salashchenko N. N., Yunin P. A., Zuev S. Y., Grazing incidence mirrors with enhanced reflectance in the soft X-ray region, Thin Solid Films, 2016, 598, 156–160.

[2] Kim J., Yokoyama H., Matsuyama S., Sano Y., Yamauchi K., Improved reflectivity of platinum/carbon multilayers for X-ray mirrors by carbon doping into platinum layer, Curr. Appl. Phys., 2012, 12, S20–S23.

[3] Wang Z., Cheng X., Zhu J., Huang Q., Zhang Z., et al., Investigation of aperiodic W/C multi-layer mirror for X-ray optics, Thin Solid Films, 2011, 519, 6712–6715.

[4] Bridou F., Delmotte F., Troussel P., Villette B., Design and fabrication of X-ray non-periodic multilayer mirrors: Apodization and shaping of their spectral response. Nucl. Instr. Meth. Phys. Res. A, 2012, 680, 69–74.

[5] Compton A.H., The total reflection of x rays, Philos. Mag., 1923, 45, 1121–1131.

[6] Kirkpatrick P., Baez A. V., Formations of optical Images by x-Ray, J. Opt. Soc. Am, 1948, 38, 766.

[7] Sauneuf R., Dalmasso J. M., Jalinaud. T., Le Breton J. P., Schirmann D. et al., Large–field high-resolution x-ray microscope for studying laser plasmas, Rev. Sci. Instrum., 1995, 68, 3412–3420.

[8] Bennett G.R., Advanced one-dimensional x-ray microscope for the Omega Laser Facility, Rev. Sci. Instrum., 1999, 70, 608–612.

[9] Hu J., Zhao L., Li X., Design and analysis of x-ray microscope of four mirrors working at grazing incidence, Proc. of SPIE, 2005, 6034, 60340M-1.

[10] Hu J., Zhao L., Li X., Wu X., Bai, Y., Imaging quality analysis of KBA x-ray microscope working at grazing incidence, Proc.of SPIE, 2004, 5638, 956–960.

[11] Liu C., Ice G. E., Liu W., Assoufid L., Qian J., et al., Tischler. Fabrication of nested elliptical KB mirrors using profile coating for synchrotron radiation X-ray focusing, Appl. Surf. Sci., 2012, 258, 2182–2186.

[12] Fouda D. A., Hamdy M., Nouh M., Beheary M., Bakrey A., et al., Model atmosphere analysis of two new early-type O4 dwarfs stars, Appl. Math. Nonlin. Sci., 2017, 2, 559-564.

[13] Motyl J., Upper separated multifunctions in deterministic and 45 stochastic optimal control, Appl. Math. Nonlin. Sci., 2017, 2, 479-484.